ELSEVIER

Physica C 362 (2001) 156–163

PHYSICA C

www.elsevier.com/locate/physc

# Interlayer tunneling of quasiparticles and Cooper pairs in Bi-2212 from experiments on small stacks

Yu.I. Latyshev [a,b,c,*], S.-J. Kim [a,c], V.N. Pavlenko [a,b], T. Yamashita [a,c], L.N. Bulaevskii [d]

[a] *Research Institute of Electrical Communication, Tohoku University, 2-1-1 Katahira, Aoba-ku, Sendai 980-8577, Japan*
[b] *Institute of Radio-Engineering and Electronics, Russian Academy of Sciences, 11-7 Mokhovaya street, GSP, Moscow 101999, Russia*
[c] *CREST, Japan Science and Technology Corporation, Japan*
[d] *Theory Division, Los Alamos National Laboratory, Los Alamos, NM 87545, USA*

Received 23 August 2000

**Abstract**

The interlayer tunneling has been studied on high quality Bi-2212 stacks of micron to the submicron lateral size. We found that low temperature and low voltage tunneling $I$–$V$ characteristics can be self-consistently described by Fermi-liquid model for a d-wave superconductor with a significant contribution from coherent interlayer tunneling. For micron-sized stacks we found very clear Fraunhofer type dependence of critical current across the stack on parallel magnetic field with periodicity corresponding to one flux quantum per elementary junction. The gap and pseudogap interplay with variation of temperature and magnetic field has been extracted from the $I$–$V$ characteristics. We consider also the role of charging effects for submicron stacks. 

*PACS:* 74.72.Hs; 74.50.+r
*Keywords:* Interlayer tunneling coherency; Gap symmetry; Pseudogap; Charging effects

## 1. Introduction

The layered structure of the most anisotropic high-$T_c$ superconductors can be considered as a stack of the elementary Josephson junctions formed between superconducting double $CuO_2$ layers separated by isolating $BiO_2$ and $SrO_2$ layers. That provides possibility of studies the interlayer tunneling of quasiparticles [1] and Cooper pairs [2]. As it was pointed out in Ref [3], to observe intrinsic Josephson effects one needs to have stacks of very small in-plane size, compared or less than Josephson penetration depth $\lambda_J = s\lambda_c/\lambda_{ab}$, where $s$ is the spacing between superconducting layers and $\lambda_c$, $\lambda_{ab}$ are anisotropic London penetration depths. The typical value of $\lambda_J$ for high-$T_c$ materials of Bi-2212 type is of the order of 1 μm. For the structure with bigger in-plane size the entering Josephson vortices can break phase coherency between the layers. Another request is a high crystallographic perfection of the structure, since defects and impurities can also break interlayer phase coherence.

* Corresponding author. Address: Institute of Radio-Engineering and Electronics, Russian Academy of Sciences, 11 Mokhovaya street, 103907 Moscow, Russia. Tel.: +7-95-203-4976; fax: +7-95-203-8414.
*E-mail address:* lat@mail.cplire.ru (Yu.I. Latyshev).

0921-4534/01/$ - see front matter 
PII: S0921-4534(01)00663-3

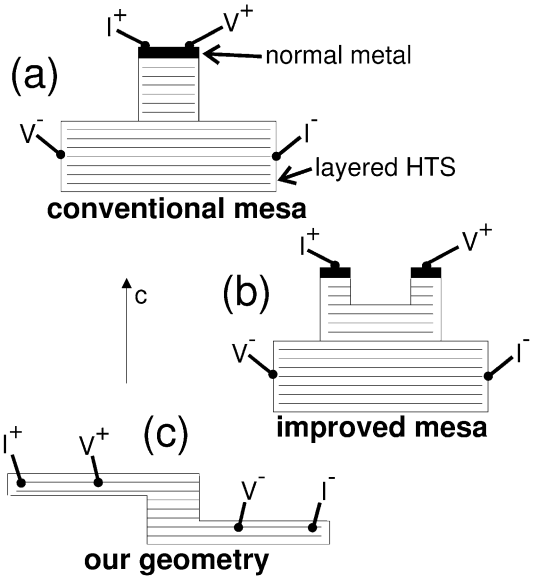


Fig. 1. Schematic view of different types of stacked structures: (a) mesa type structure, (b) improved mesa structure and (c) double step structure.

The mesa-type structures, shown in Fig. 1a, have been widely used in the studies of interlayer tunneling [4–6]. Structures of this type have some disadvantages: troubles with separation of top electrodes for four-probe measurements; the injection of quasiparticles from normal metal top electrode that drives system into non-equilibrium state, etc. To avoid quasiparticle injection more complicated mesas have been constructed (Fig. 1b) [7], however the lateral size of that type structures still remained relatively big, within 2–3 μm.

We elaborated a new type of double step stacked structures [8], shown in Fig. 1c. In this configuration both electrodes are superconducting. Also there is no principal limitations for the lateral size of the structure, since electrical contacts are located beyond the junction region. As a base material for stack fabrication we used single crystal Bi-2212 whiskers. Using focused ion beam (FIB) technique we fabricated stacked structures with lateral sizes down to submicron level [9]. In this paper we review our last results on interlayer tunneling in those small stacks.

## 2. Experimental

Bi-2212 single crystal whiskers have been grown by impurity free method [10]. Thin whiskers have been characterized as a very perfect crystalline materials [10]. They grow along the *a*-axis free of any crucible or substrate and can be entirely free of macroscopic defects and dislocations. In the *bc*-plane they have rectangular cross-section. The typical sizes of whisker are $L_a = 100$–$500$ μm, $L_b = 1$–$10$ μm, $L_c = 0.1$–$1$ μm.

For the fabrication of stacked junction we used the conventional FIB machine of Seiko Instruments Corp., SMI 9800 (SP) with $Ga^+$-ion beam. The junctions have been fabricated by double-sided processing of whisker with FIB. The details of fabrication steps are described in Ref. [9]. Four Ag contact pads have been evaporated and annealed before FIB processing to avoid Ga-ions diffusion into the junction body. Parameters of the stacks are listed in the Table 1.

Table 1
Parameters of Bi-2212 stacked junctions

| No. | $S$ (μm$^2$) | $N$ | $V_g$ (V) | $I_c$ (μA) | Notes |
|---|---|---|---|---|---|
| 1 | 0.4 | 70 | 2.4 | 0.1 | |
| 2 | 2.0 | 65 | 1.3 | 12 | |
| 3 | 1.5 | 50 | 1.1 | 6 | |
| 4 | 0.6 | 35 | 1.7 | 0.25 | |
| 5 | 0.3 | 50 | 2.2 | 0.07 | |
| 6 | $36 \times 0.5$ | 50 | 3.0 | 14 | Array $6 \times 6$ junctions |
| 7 | 400 | 40 | 0.8 | 1000–2000 | Data taken from Ref. [1] |
| 8 | 0.4 | 70 | 2.4 | ~0.05 | |
| H-1 | 2.0 | 35 | 1.4 | 0.6 | Contains a hole $D = 0.2$ μm |

### 2.1. Low temperature and voltage I–V characteristics

Fig. 2(b) and (c) shows the $I$–$V$ characteristics of samples #3 and #4 respectively. The fully superconducting overlap geometry of the stack (Fig. 2a) was used to suppress the effects of quasiparticle injection on the tunneling characteristics [1,11]. We also substantially reduced the effects of self-heating in our submicron mesa junctions [12,13]. Self-heating manifests itself as the S-shaped $I$–$V$ curve near the gap voltage of the stack $V_g$.

The measured temperature dependence of the $c$-axis resistivity of the stack was typical for slightly overdoped Bi-2212 crystals with $T_c \approx 77$ K [14].

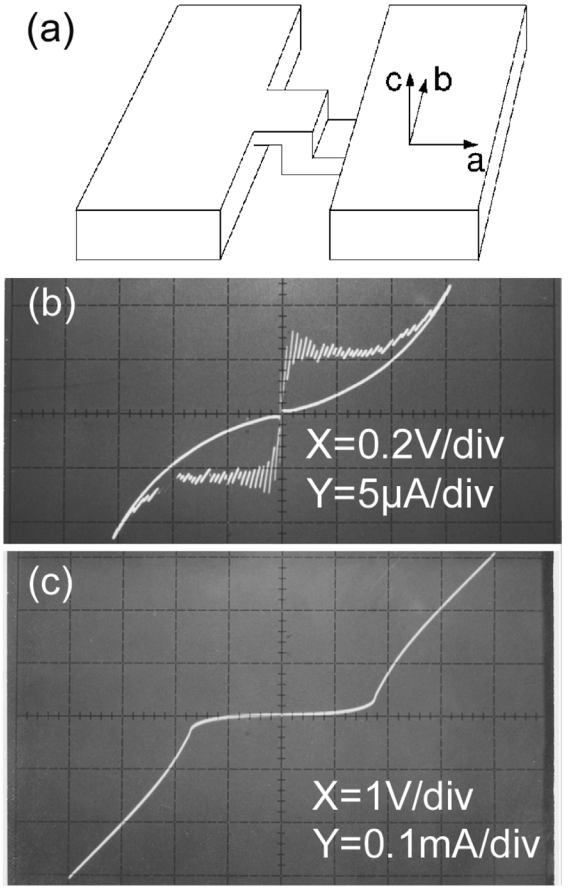


Fig. 2. Schematic view of the junction (a); and the $I$–$V$ characteristics of the Bi-2212 stacks in (b) enlarged scale for sample #3 and (c) extended scale for sample #4. $T = 4.2$ K.

The superconducting gap (pseudogap) voltage of the stack, $V_g$, was determined from the $I$–$V$ characteristics as the voltage at the maximum of the $dI/dV(V)$. The gap of the intrinsic junction, $2\Delta_0 \approx eV_g/N$, where $N$ is the number of elementary layers in the stack, reaches value as high as 50 meV (see Refs. [12,13]). The multibranched structure, which is clearly seen in Fig. 2b corresponds to subsequent transition of the intrinsic junctions into the resistive state for increasing voltage [15]. At voltages $V > V_g$ all junctions are resistive. In downsweep of voltage, starting from $V > V_g$ the $I$–$V$ curve is observed in the all junction resistive state. Here, only quasiparticles contribute to the $c$-axis transport. Corresponding quasiparticle conductivity, $\sigma_q$, thus can be defined directly from that part of the $I$–$V$ curve. The Ohmic resistance, $R_n$, at $V > V_g$ is well defined (Fig. 2c). This resistance is nearly temperature independent (Fig. 3) and corresponds to the conductivity $\sigma_n(V > V_g) \approx 80$ $(k\Omega cm)^{-1}$ for energies above superconducting gap and pseudogap. The critical current $I_c$ was determined from the $I$–$V$ characteristics as the current of switching from the superconducting to the resistive state, averaged over the stack. The variation of the critical current along the stack is not large (usually within 15%), indicating a good uniformity

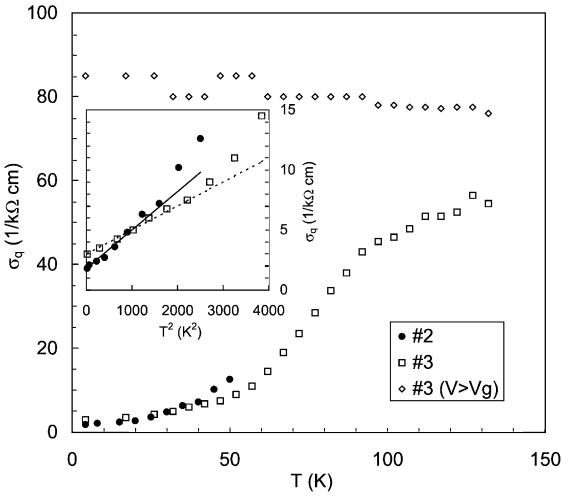


Fig. 3. Quasiparticle dynamic conductivity $\sigma_q$ vs $T$ for voltages $v > V_g/N \approx 2\Delta_0/e$ and $v = V/N \to 0$, as extracted from the $I$–$V$ characteristics of samples #2 and #3. The insert shows $\sigma_q$ vs $T^2$ at $v \to 0$. Lines are fit for $T^2 < 1000$ K$^2$.

of our structures. The $c$-axis critical current density, $J_c$, for the junctions with in-plane area $S > 2\ \mu m^2$ was typically 600 A/cm$^2$ at $T = 4.2$ K [12,13].

We found out that interlayer tunneling $I$–$V$ characteristics at low temperatures essentially differ from those of conventional Josephson junctions between s-wave superconductors. We specify [16]: (1) strong disagreement with Ambegaokar–Baratoff (A–B) relation, $J_c^{AB}(0) = \pi\sigma_n\Delta_0/2es$, with $s$ the spacing between intrinsic superconducting layers (15.6 Å); (2) quadratic dependences of quasiparticle conductivity $\sigma_q(V,T)$ on $V$ and $T$ (Figs. 3 and 4): $\sigma_q(V,0) = \sigma_q(0,0)(1+\alpha V^2)$, $\sigma_q(0,T) = \sigma_q(0,0)(1+\beta T^2)$ with $\alpha = 0.014 \pm 0.003$ (meV)$^{-2}$, $\beta = (6 \pm 2) \times 10^{-4}$ K$^{-2}$, (3) nonzero and universal value of $\sigma_q(0,0) \approx 2$ (kΩcm)$^{-1}$.

We found empirically the modified relation of the A–B type,

$$J_c(0) \approx \pi\sigma_q(0,0)\Delta_0/2es \tag{1}$$

and scaling relation between $\alpha$ and $\beta$, $\beta/\alpha =$ const. $\approx 4 \pm 2$. It was shown that all these features can be described self-consistently by Fermi-liquid model for quasiparticles in clean d-wave superconductor with resonant scattering [16]. Impurity scattering leads to the formation of gapless state

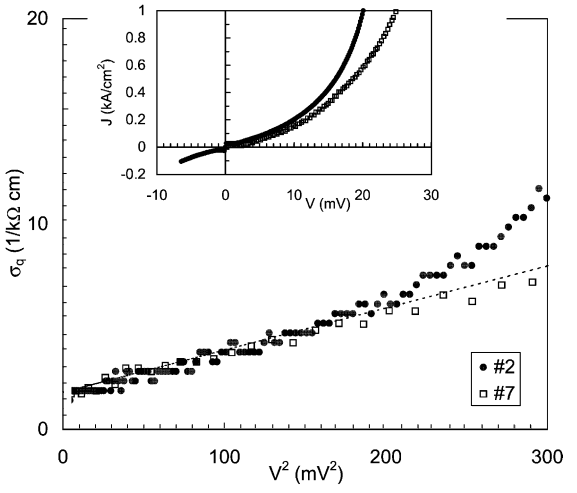


Fig. 4. Quasiparticle differential conductivity $\sigma_q$ vs $v^2 = V^2/N^2$ at $T = 4.2$ K as extracted from the $I$–$V$ characteristics of samples #2 and #7 (from Ref. [1]). Line is fit for $v < 10$ mV. Insert shows corresponding $J$–$v$ characteristics.

near the node directions $\varphi_g$ at angles $\varphi_g \pm \varphi_0/2$, with $\varphi_0 \sim \gamma/\Delta_0$ where $\gamma$ is the impurity bandwidth of quasiparticles. That results in a nonzero density of states at zero energy, $N(0)\varphi_0$, where $N(0)$ is the 2D density of states per spin at the Fermi level, and leads to a universal quasiparticle interlayer conductivity $\sigma_q(0,0)$. It was shown also [16] that the values of $\sigma_q(0,0)$, $J_c(0)$ and coefficients $\alpha$ and $\beta$ are strongly dependent on the coherency of interlayer tunneling. If to denote the weight for in-plane momentum conserving (coherent) tunneling as $a$ and for incoherent as $(1-a)$, the ratio $J_c(0)/\sigma_q(0,0)$ is expressed as follows [16]

$$J_c(0)/\sigma_q(0,0) = (\pi\Delta_0/2es)[a + (1-a)\Delta_0/\varepsilon_F] \\ /[a + (1-a)\gamma/\varepsilon_F] \tag{2}$$

with $\varepsilon_F$ the Fermi energy. Correspondingly for coefficients $\alpha$ and $\beta$ it was obtained [16]

$$\alpha \approx 1/8\gamma^2[1 + (1/a - 1)\gamma/\varepsilon_F], \\ \beta \approx \pi^2/(18\gamma^2)[1 + (1/a - 1)\gamma/\varepsilon_F]. \tag{3}$$

One can see that Eq. (2) turns to the experimentally found relation (1) only for significant contribution of coherent tunneling, $a \gg \max\{\Delta_0/\varepsilon_F, \gamma/\varepsilon_F\}$. From experimental value for $\beta$ we can estimate $\gamma$ from Eq. (3) to be $\gamma \approx 3$ mV. Then for $\Delta_0/\varepsilon_F \approx 0.1$ we can get estimation for $a$, $a \gg 0.1$. Eq. (3) gives $\beta/\alpha = 4\pi^2/9$ when a $\to 1$ in a reasonable agreement with experiment.

Thus our low $V$, low $T$ tunneling data are consistent with Fermi-liquid picture taking into account d-wave symmetry and considerably coherent interlayer tunneling. This is an agreement with the angle-resolved photoemission spectroscopy (ARPES) data [17] where quasiparticle peak has been observed at low temperatures.

### 2.2. DC intrinsic Josephson effect

Earlier a dimensional crossover for observation of DC intrinsic Josephson effect was found [8]. The oscillatory dependence $I_c(H)$ began to appear for stacks with in-plane size less than 10–20 μm. Here we studied DC intrinsic Josephson effect at much smaller scale of $L$ down to 1 μm. That corresponds to the limit when $L$ becomes smaller than the size of Josephson vortices, $2\lambda_J$, which we estimate for

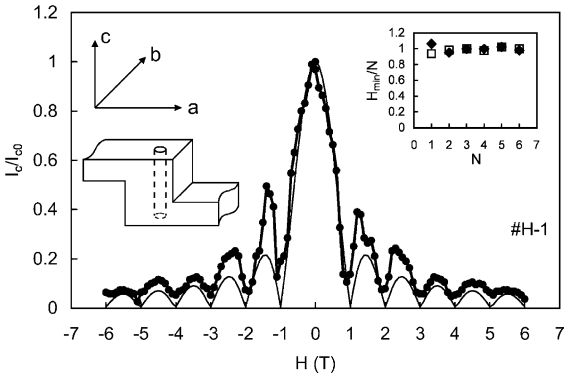


Fig. 5. Dependence of normalized critical current across the layers $I_c/I_{c0}$ on parallel magnetic field $H$ for sample H-1 at 4.2 K. Thin solid line is a fit to Fraunhofer dependence $\sin x/x$, $x = \pi sLH/\Phi_0$ for $L = 1.4$ μm. The left insert shows schematically the junction geometry. The right insert shows that a period of oscillations does not depend on oscillation number $N$ and $H$, $-H$ orientation.

our case to be 2–3 μm. The major part of small junctions had reduced critical current density (by factor 3–10) and suppressed hysteresis of the $I$–$V$ characteristics. It may be a result of damage of the edge parts of the stack by FIB processing.

Fig. 5 shows a dependence of the normalized critical current on parallel magnetic field of the sample #H-1 with a size $L = 1.4$ μm. This sample contained a small hole at the center (see insert to Fig. 5). The samples with hole have no hysteresis of the $I$–$V$ characteristics at low bias voltage. The critical current was measured as a sharp transition into resistive state with bias increasing. At zero magnetic field that corresponds to the switch in resistive state of about 10% of the total number of junctions in the stack. The number of synchronized junctions was increased in parallel magnetic field: up to 30% at $H = 0.6$ T, to 50% at $H = 1.5$ T and to 80% at $H = 3$ T as was estimated by the resistance after switch from superconducting to appropriate ohmic resistive state. That may be the reason of much better fit of experimental dependence $I_c(H)$ to theoretical one at $H > 3$ T.

Actually the experimental dependence follows quite well the theoretical Fraunhofer dependence $I_c/I_{c0} = |\sin x/x|$, with $x = \pi LsH/\Phi_0$, where $\Phi_0$ is a flux quantum. Six periods of $I_c(H)$ oscillations have been clearly observed for both parallel and anti-parallel field orientation. The value of experimentally found period $\Delta H_{exp} = 1 \pm 0.02$ T within accuracy of 1–2% coincide with theoretical value, $\Delta H = \Phi_0/Ls$ for $L = 1.4$ μm, $s = 15.6$ Å. The H, $-$H symmetry of $I_c(H)$ dependence indicates the absence of the trapped flux.

We did not study carefully micron sized stacks without hole. However, preliminary results show that oscillations of $I_c(H)$ appears at that type of junctions as well in magnetic fields exceeding the field which completely suppresses hysteresis of the $I$–$V$ characteristics at low biasing.

Fig. 5 demonstrates the real capability of fabrication of nanoscale quantum interference device. Note that the scale of period, ~1 T, is about four orders higher than observed in conventional Josephson junctions.

### 2.3. Charging effects

As is well known, the Josephson tunneling can be suppressed by the Coulomb blockade effect in small junctions [18], when the charging energy $E_c$ becomes comparable with the Josephson coupling energy $E_J$ provided that the normal state resistance exceeds so called quantum resistance $R_Q = h/4e^2$. The charging effects become even more significant in arrays of small junctions [19]. The $c$-axis junction fabricated from layered high-$T_c$ material is in fact the vertically stacked array of elementary tunnel junctions. Therefore, one can expect an appearance of substantial charging effects in such a structure with decreasing of its in-plane size. Until recently the fabrication of the high-$T_c$ stacks was limited by the in-plane size ~2 μm and no charging effects have been detected. We report here on our recent search of charging effects in Bi-2212 submicron stacks.

For the submicron junctions we clearly observed tunneling characteristics with superconducting gap (~50 meV per elementary junction) (Fig. 2c). We found also a number of new features. The $I$–$V$ characteristics have no hysteresis and multibranched structure, the critical current has a finite slope decreasing with temperature, the periodic structure of current peaks develops on the $I$–$V$ curves at low temperatures (Fig. 6a), and $J_c(0)$ is reduced [12,13]. Formally, all these details re-

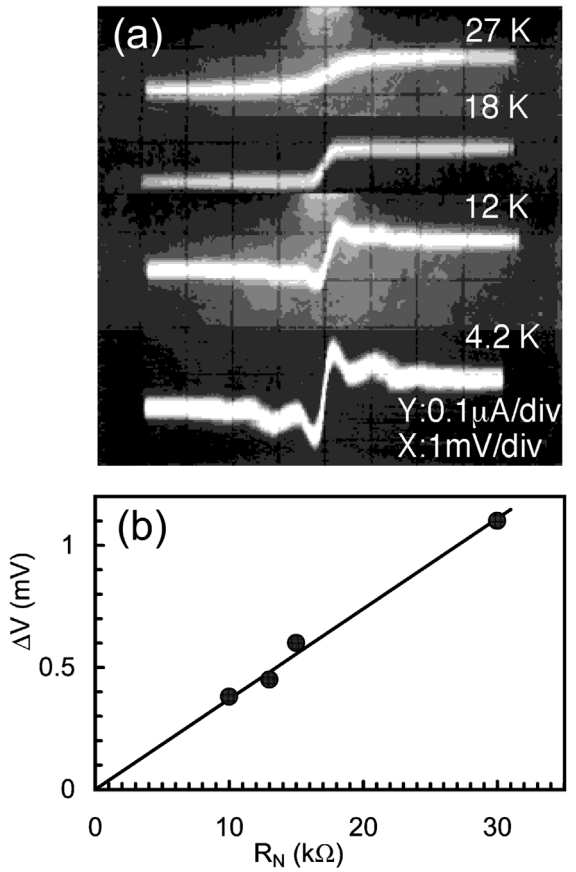


Fig. 6. Extended scale $I$–$V$ characteristics of submicron Bi-2212 stack #5 for different temperatures (a) and dependence of the period of current peak structure $\Delta V$ on the normal state resistance $R_n$ for four different submicron stacks (b).

semble the features typical for the single Cooper pair tunneling in small tunnel junctions [20]. The period of observed Coulomb staircase $\Delta V$ corresponds to the charge energy of the stack [12,13] $E_c = e^2/C$, with $C$ the net capacitance of the stack $C = C_0/N$. $C_0$ is a capacitance of elementary junction. We found for various stacks that the period $\Delta V$ is indeed proportional to $1/C$ or $R_n$ (Fig. 6b). We used here that the product $R_qC$ is a constant independent of sample geometry [12,13] and also that the ratio $R_q/R_n$ is a constant equal $\approx$30 at 4.2 K [16].

The other two requirements for observation of the charging effects are related to the smallness of quantum and thermal fluctuations preventing Coulomb blockade. To avoid quantum fluctuations the interlayer tunneling resistance $R_q = s/(\sigma_q S)$ should be high enough: $R_q/N > R_Q$ [21]. That can be rewritten for $R_n/N$ at low temperatures as follows $R_n/N > R_Q/30 \approx 0.2$ kΩ. This condition has been satisfied for all the stacks showing the features of charging effects at low temperatures.

Thermal fluctuations become significant at high temperatures when energy of thermal fluctuations, $kT$, exceeds charging energy. For #5 it happens at temperatures above 12 K. This is consistent with our observations. As it follows from Fig. 6a the Coulomb staircase structure of current peaks gradually washes out and disappears above 18 K.

As it was mentioned above a dimensional crossover to the Coulomb blockade regime occurs when charging energy becomes comparable with the Josephson coupling energy. The net Josephson energy of the stack $E_J$ is also proportional to the number of the elementary junctions in the stack as $E_c$. Thus a condition for a crossover does not depend on the number of junctions $N$ and can be rewritten for a one elementary junction: $4E_{c0} = E_{J0}$ [18]. From this condition we can get expression for the junction area corresponding to the crossover $S = 16\pi^2 es\lambda_c/(\Phi_0\varepsilon_c^{1/2})$ where $\varepsilon_c$ is interlayer dielectric constant. For Bi-2212 that corresponds to $S \approx 0.1$ μm$^2$ i.e. significant charging effects should be observed for junction $0.3 \times 0.3$ μm$^2$. This estimation is not far from experimental conditions.

### 2.4. Gap and pseudogap spectroscopy

The interlayer tunneling $I$–$V$ characteristics in small stacked junctions provide an important possibility of gap and pseudogap spectroscopy in layered high-$T_c$ cuprates. In comparison with other widely used methods for gap and pseudogap studies like ARPES or scanning tunneling microscopy (STM) (see as a review Ref. [22]) which are in fact surface methods, the interlayer tunneling spectroscopy gets an information from the body of the single crystal. Our submicron Bi-2212 stacks show high quality tunneling characteristics. Both the gap and the pseudogap are clearly seen in the first derivatives of the $I$–$V$ characteristics (Fig. 7). Fig. 8a shows the related temperature

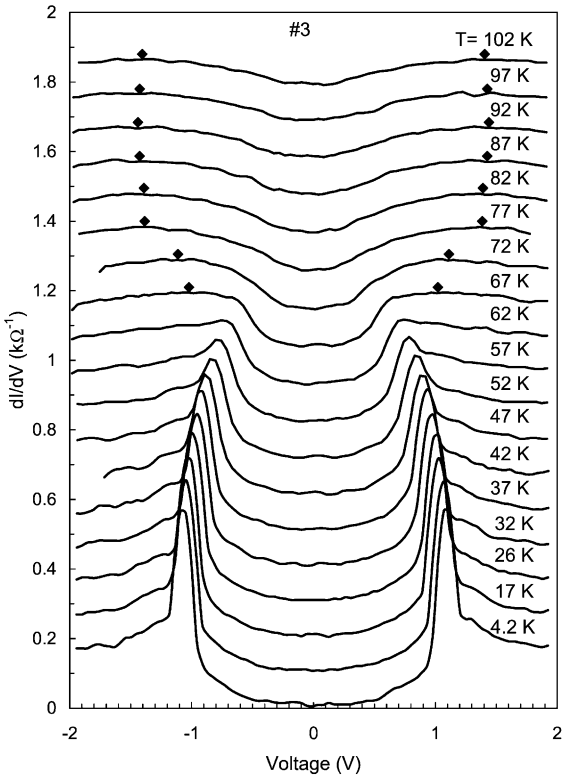


Fig. 7. Differential conductivity $dI/dV$ as a function of the voltage bias $V$ of Bi-2212 stack #3 for various temperatures ranging from 4.2 to 102 K. The curves are shifted for clarity. The scale corresponds to the lowest curve. The pseudogap position is marked by rhombuses.

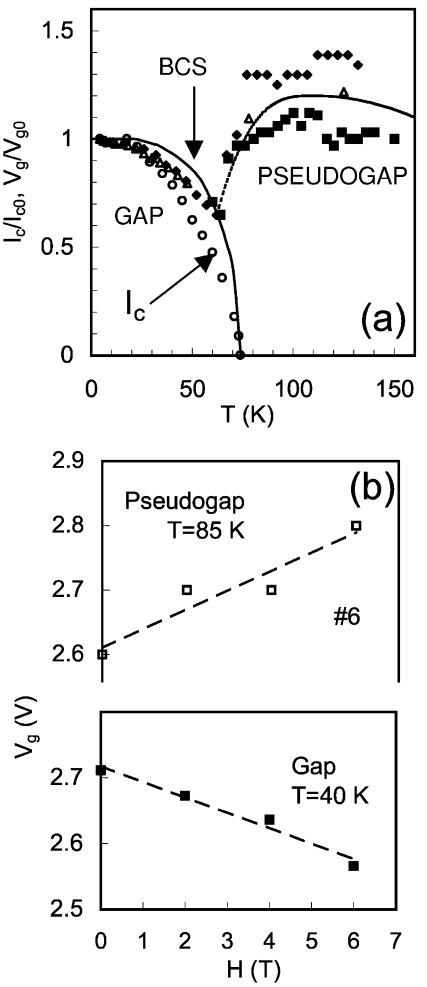


Fig. 8. Gap and pseudogap dependences on temperature (a) and magnetic field $H\|c$ (b). Denotes of the panel (a) correspond to the following samples: (◆) – #3, (△) – #8, (■) – #1. Line for pseudogap temperature dependence is guide to eye.

dependence of gap and pseudogap. Starting from low temperatures a gap goes down more rapidly than usual BCS dependence (solid line). We defined $T_c$ at a point (77 K) where $I_c(T)$ turns to zero. At $T > 65$ K the gap evolves into the pseudogap that was observed up to 160 K. The maximum pseudogap value $2\Delta_p$ at ~110 K is about 20% higher than superconducting gap $2\Delta_0$. We have never observed simultaneously a gap and a pseudogap at the interval $65 < T < 77$ K. The most interesting observed feature is that the pseudogap abruptly goes down approaching $T_c$ from high temperatures. It may be an indication of the anti-coexistence of the gap and the pseudogap. That type of temperature behavior has been reproduced recently on break Bi-2212 junctions [23], but is in conflict with STM measurements on Bi-2212 [24], where neither gap nor pseudogap variation with temperature has been reported. We have undertaken also the studies of the gap and pseudogap dependences on magnetic field $H\|c$ up to 6 T (see Fig. 8b). We found that the gap is suppressed by magnetic field. To the contrast the pseudogap is enhanced by $H$ (Fig. 8b). That observation, to our opinion, excludes pseudogap origin due to superconducting fluctuations [25] or due to existence of preformed Cooper pairs [26] above $T_c$ and points out to the different origin of ordering for the gap and for the pseudogap formation. Our results were obtained on slightly

overdoped Bi-2212 samples [27]. Similar behavior of pseudogap on temperature and magnetic field has been recently obtained for Bi-2212 mesas with oxygen variation from overdoped to underdoped regime [28]. In recent experiments on the underdoped Bi-2212 [29] the gap and pseudogap have been observed simultaneously on the $I$–$V$ characteristics of Bi-2212 stacks below $T_c$.

## 3. Conclusions

We studied interlayer tunneling on small stacked junctions. The results obtained point out to the d-wave symmetry of order parameter, to the significant contribution from coherent interlayer tunneling, to the "non-superconducting" origin of the pseudogap. We uncovered also the influence of charging effects on interlayer tunneling in submicron stacks.

*Note:* A paper by A. Irie et al. [30] has appeared recently where on Bi-2212 mesa with in-plane size of $1.2 \times 1.2$ μm$^2$ and $\lambda_J \sim 1$ μm the critical currents of all 12 constituent junctions have shown the magnetic field dependence close to the Fraunhofer pattern similar to our data.

## Acknowledgements

The work has been done in collaboration with Los Alamos National Lab. We are thankful to M.J. Graf, A.V. Balatsky, M. Maley and N. Morozov for cooperation. We thank A.M. Nikitina for providing us with Bi-2212 single crystal whiskers. This work was supported by the Russian State Program on HTS under grant no. 99016.

## References

[1] K. Tanabe, Y. Hidaka, S. Karimoto, M. Suzuki, Phys. Rev. B 53 (1996) 9348.
[2] R. Kleiner, F. Steinmeyer, G. Kunkel, P. Müller, Phys. Rev. Lett. 68 (1992) 239.
[3] L.N. Bulaevskii, J.R. Clem, L.I. Glazman, Phys. Rev. B 46 (1992) 350.
[4] F.X. Regi, J. Schneck, H. Savary, R. Mellet, P. Müller, R. Kleiner, J. Phys. III (France) 4 (1994) 2249.
[5] A. Yurgens, D. Winkler, Y.M. Zang, N. Zavaritsky, T. Claeson, Physica C 235–240 (1994) 3269.
[6] P. Seidel, F. Schmidt, A. Pfuch, H Schneidewind, E. Heinz, Proc. 5th Int. Supercond. Electron. Conf. (ISEC'95), Nagoya, Japan, 1995 (Inst. of Physics Publishing, Bristol, 1996, p. 63).
[7] A. Yurgens, D. Winkler, T. Claeson, G. Yang, I.F.G. Parker, C.E. Gough, Phys. Rev. B 59 (1999) 7199.
[8] Yu.I. Latyshev, J.E. Nevelskaya, P. Monceau, Phys. Rev. Lett. 77 (1996) 932.
[9] Yu.I. Latyshev, S.-J. Kim, T. Yamashita, IEEE Trans. Appl. Supercond. 9 (1999) 4312.
[10] Yu.I. Latyshev, I.G. Gorlova, A.M. Nikitina, V.U. Antokhina, S.G. Zybtsev, N.P. Kukhta, V.N. Timofeev, Physica C 216 (1993) 471.
[11] A. Yurgens, D. Winkler, N.V. Zavaritsky, T. Claeson, Phys. Rev. B 53 (1996) R8887.
[12] Yu.I. Latyshev, S.-J. Kim, T. Yamashita, JETP Lett. 69 (1999) 84.
[13] Yu.I. Latyshev, S.-J. Kim, T. Yamashita, JETP Lett. E. 69 (1999) 640.
[14] T. Watanabe, T. Fujii, A. Matsuda, Phys. Rev. Lett. 79 (1997) 2113.
[15] R. Kleiner, P. Müller, Phys. Rev. B 49 (1994) 1327.
[16] Yu.I. Latyshev, T. Yamashita, L.N. Bulaevskii, M.J. Graf, A.V. Balatsky, M.P. Maley, Phys. Rev. Lett. 82 (1999) 5345.
[17] M.R. Norman, H. Ding, M. Randeria, J.C. Campuzano, T. Yokoya, T. Takeuchi, T. Mochiku, K. Kadowaki, P. Guptasarma, D.G. Hinks, Nature (London) 392 (1998) 6672.
[18] M. Tinkham, Introduction to Superconductivity, Mc Graw-Hill, New York, 1996 (Chapter 7).
[19] P. Delsing in: H. Grabert, M.H. Devoret (Eds.), Single Charge Tunneling, Plenum Press, New York, 1992, pp. 249–274.
[20] D.B. Haviland, Y. Harada, P. Delsing, C.D. Chen, T. Claeson, Phys. Rev. Lett. 73 (1994) 1541.
[21] L.N. Bulaevskii, A.E. Koshelev, M.P. Maley, preprint.
[22] T. Timusk, B.W. Statt, Rep. Prog. Phys. 62 (1999) 61–122.
[23] T. Ekino, Y. Sezaki, H. Fujii, Phys. Rev. B 60 (1999) 6916–6922.
[24] Ch. Renner, B. Revaz, J.-Y. Genoud, K. Kadowaki, O. Fisher, Phys. Rev. Lett. 80 (1998) 149–152.
[25] A.M. Cucolo, M. Cuoco, A.A. Varlamov, Phys. Rev. B 59 (1999) R11675.
[26] Q. Chen, I. Kostin, B. Janky, K. Levin, Phys. Rev. Lett. 81 (1998) 4708.
[27] Yu.I. Latyshev, V.N. Pavlenko, S.-J. Kim, T. Yamashita, in: T. Yamashita, K. Tanabe (Eds.), Advances in Superconductivity XII, Proc. 12th Int. Symp. Supercond., ISS'99, October 17–19, 1999, Morioka, Springer, 2000, pp. 47–52.
[28] P. Müller, S. Rother, O. Waldmann, S. Heim, M. Mößle, R. Kleiner, preprint.
[29] V.M. Krasnov, A. Yurgens, D. Winkler, P. Delsing, T. Claeson, Phys. Rev. Lett. 84 (2000) 5860.
[30] A. Irie, S. Heim, S. Schromm, M. Mößle, T. Nachtrab, M. Gódo, R. Kleiner, P. Müller, G. Oya, Phys. Rev. B 62 (2000) 6681.